Inorg. Chem. **2003**, *42*, 7616–7625

Molecular Metamagnet $[Ni(4ImNNH)_2(NO_3)_2]$ (4ImNNH = 4-Imidazolyl Nitronyl Nitroxide) and the Related Compounds Showing Supramolecular H-Bonding Interactions

Chigusa Aoki, Takayuki Ishida,* and Takashi Nogami

Department of Applied Physics and Chemistry, The University of Electro-Communications, Chofu, Tokyo 182-8585, Japan

Received July 30, 2003

A new chelating radical ligand 4ImNNH (2-(4-imidazolyl)-4,4,5,5-tetramethylimidazolin-1-oxyl 3-oxide) was prepared, and complexation with divalent transition metal salts gave complexes, $[M(4ImNNH)_2X_2]$, which showed intermolecular ferromagnetic interaction in high probability (7 out of 10 paramagnetic compounds investigated here). The nitrate complexes (X = NO_3; M = Mn (**1**), Co (**2**), Ni (**3**), Cu (**4**)) crystallize isomorphously in monoclinic space group $P2_1/a$. The equatorial positions are occupied with two 4ImNNH chelates and the nitrate oxygen atoms are located at the axial positions. Magnetic measurements revealed that the intramolecular exchange couplings in **1**, **2**, and **4** were antiferromagnetic, while that in **3** was ferromagnetic with $2J/k_B = +85$ K, where the spin Hamiltonian is defined as $H = -2J(S_1 \cdot S_2 + S_2 \cdot S_3)$ based on the molecular structures determined as the linear radical–metal–radical triads. The intramolecular ferromagnetic interaction in **3** is interpreted in terms of orthogonality between the radical π^* and metal dσ orbitals. Compounds **1**–**3** exhibited intermolecular ferromagnetic interaction ascribable to a two-dimensional hydrogen bond network parallel to the crystallographic *ab* plane. Complex **3** became an antiferromagnet below 3.4 K and exhibited a metamagnetic transition on applying a magnetic field of 5.5 kOe at 1.8 K. The complexes prepared from metal halides, $[M(4ImNNH)_2X_2]$ (X = Cl, Br; M = Mn, Co, Ni, Cu), showed intramolecular antiferromagnetic interactions, which are successfully analyzed based on the radical–metal–radical system. The crystal structures determined here on **1**–**4**, $[Mn(4ImNNH)_2Cl_2]$, and $[Cu(4ImNNH)_2Br_2]$ always have intermolecular hydrogen bonds of H(imidazole)···X(axial ligand)–M, where X = NO_3, Cl, Br. This interaction seems to play an important role in molecular packing and presumably also in magnetic coupling.

Introduction

Polymeric complex formation containing transition metal ions and bridging radical ligands is supposed as an important strategy for constructing ferri- and ferromagnetic networks with dimensionality.[1−3] The nitronyl nitroxide (4,4,5,5-tetramethylimidazolin-1-oxyl 3-oxide; abbreviated as NN hereafter) family has been widely utilized because of their bidentate nature suitable for bridge formation[1] (Chart 1). In addition, intermolecular ferromagnetic couplings are often observed in NN radical crystals,[4−8] and it holds also for the metal−radical materials possessing the NN group as a peripheral substituent.[9] The role of hydrogen (H) bonds has been discussed in connection with ferromagentic exchange

* Author to whom correspondence should be addressed. E-mail: ishi@pc.uec.ac.jp.

(1) Caneschi, A.; Gatteschi, D.; Rey, P.; Sessoli, R. *Acc. Chem. Res.* **1989**, *22*, 392.
(2) Inoue, K.; Hayamizu, T.; Iwamura, H.; Hashizume, D.; Ohashi, Y. *J. Am. Chem. Soc.* **1996**, *118*, 1803. Stumpf, H. O.; Ouahab, L.; Pei, Y.; Grandjean, D.; Kahn, O. *Science* **1993**, *261*, 447. Ise, T.; Ishida, T.; Hashizume, D.; Iwasaki, F.; Nogami, T. *Inorg. Chem.* **2003**, *42*, 6106.
(3) Miller, J. S.; Epstein, A. J. *Angew. Chem., Int. Ed. Engl.* **1994**, *33*, 385. Fujita, W.; Awaga, K.; Takahashi, M.; Takeda, M.; Yamazaki, T. *Chem. Phys. Lett.* **2002**, *362*, 97.
(4) Kinoshita, M.; Turek, P.; Tamura, M.; Nozawa, Y.; Shiomi, D.; Nakazawa, Y.; Ishikawa, M.; Takahashi, M.; Awaga, K.; Inabe, T.; Maruyama, Y. *Chem. Lett.* **1991**, 1225.
(5) Sugawara, T.; Matsushita, M. M.; Izuoka, A.; Wada, N.; Takeda, N.; Ishikawa, M. *J. Chem. Soc., Chem. Commun.* **1994**, 1723. Matsushita, M. M.; Izuoka, A.; Sugawara, T.; Kobayashi, T.; Wada, N.; Takeda, N.; Ishikawa, M. *J. Am. Chem. Soc.* **1997**, *119*, 4369.
(6) Cirujeda, J.; Mas, M.; Molins, E.; Panthou, F. L.; Laugier, J.; Park, J. G.; Paulsen, C.; Rey, P.; Rovira, C.; Veciana, J. *J. Chem. Soc., Chem. Commun.* **1995**, 709. Cirujeda, J.; Ochando, L. E.; Amigo, J. M.; Rovira, C.; Rius, J.; Veciana, J. *Angew. Chem., Int. Ed. Engl.* **1995**, *34*, 55. Hernandez, E.; Mas, M.; Molis, M. E.; Rovira, C.; Veciana, J. *Angew. Chem., Int. Ed. Engl.* **1993**, *32*, 882.
(7) Yoshioka, N.; Irisawa, M.; Mochizuki, Y.; Kato, T.; Inoue, H.; Ohba, S. *Chem. Lett.* **1997**, 251.
(8) Doi, K.; Ishida, T.; Nogami, T. *Chem. Lett.* **2003**, 544.

10.1021/ic0349048 CCC: $25.00
Published on Web 10/16/2003

Chart 1

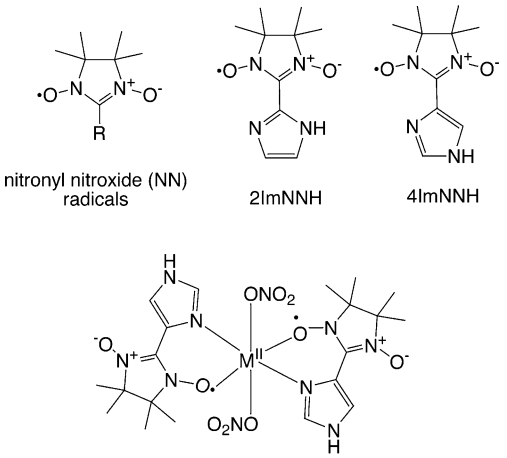

pathways.[5−8] Rey and co-workers reported the anionizable radical ligand, 2ImNNH (2-imidazolyl NN; ImH denotes imidazole), which was applied to the formation of two-dimensional magnetic materials as the anionic form.[10] We designed an isomeric radical ligand, 4ImNNH (4-imidazolyl NN), which affords networking directions different from those of 2ImNNH. Actually, the direction of H-bonds from the 4-imidazolyl NH group is quite important for the present study.

We have studied the crystal structures and magnetic properties of [M(4ImNNH)$_2$(NO$_3$)$_2$] (M = Mn (**1**), Co (**2**), Ni (**3**), Cu (**4**)) and preliminarily reported the intramolecular ferromagnetic coupling in **3** between nickel(II) and radical spins.[11] There have been ample examples of ferrimagnets[1,2] according to the metal−radical approach.[1] However, the magnets based on genuine ferromagnetic coupling are rare.[12] In addition to the issue on the intramolecular interaction, **3** also showed intermolecular ferromagnetic interaction.[11] To investigate the intermolecular magneto-structure relationship as well as intramolecular one, we prepared chloride and bromide series [M(4ImNNH)$_2$X$_2$] (M = Mn, Co, Ni, Cu (**5**−**8** for X = Cl; **9**−**12** for X = Br)) and found that seven compounds exhibited intermolecular ferromagnetic interaction. We will report here the structural and magnetic characterization of **1**−**12**.

Experimental Section

Materials. The NN-substituted ligand 4ImNNH was prepared according to Ullman's method[13] by using 4-formylimidazole as a starting material. The precursor bishydroxyimidazoline was obtained in 27% yield from 4-formylimidazole, and the treatment with $NaIO_4$ in water gave 4ImNNH as dark blue polycrystals in 37% yield from the bishydroxyimidazoline, mp 154−160 °C (CH_2Cl_2-hexane). The ESR spectrum measured on a Bruker ESP300E supports the presence of the nitronyl nitroxide group. The spectrum shows a 1:2:3:2:1 quintet pattern with $g = 2.0066$ and $a_N = 7.59$ G in toluene at room temperature.

The following complexation procedure is typical. An ethanol solution (2.5 mL) containing $Ni(NO_3)_2 \cdot 6H_2O$ (30.2 mg, 0.104 mmol) and 4ImNNH (44.8 mg, 0.201 mmol) was allowed to stand in a refrigerator for a week. The resultant black crystals of **3** were collected on a filter and washed with a small amount of water, which are suitable for X-ray crystal structure and magnetic studies. The yield of **3** was 59.7 mg (94%). Similarly, other complexes were obtained in good yields (typically about 90% for X = NO_3, 80% for X = Cl, and about 60% for X = Br), using the corresponding metal salts as starting materials. For preparation of single crystals of **4**, methanol was used as a solvent because only poorly resolved crystals were obtained from ethanol. Elemental analyses (C, H, N) on a Fisons EA-1108 by a usual combustion method supported the formulas of [M(4ImNNH)$_2$X$_2$] in the 0.3% range.

X-ray Crystallography. Diffraction data of single crystals of 4ImNNH, **1**−**4**, **5**, and **12** were collected on a Rigaku R-axis RAPID diffractometer with graphite monochromated Mo Kα radiation (λ = 0.71069 Å) at 90 K for 4ImNNH and 100 K for the coordination compounds. The structures were directly solved by a heavy-atom Patterson method or the SIR program[14] in the teXsan program package.[15] Numerical absorption correction was used. All of the hydrogen atoms could be found in difference Fourier maps, and the parameters of the hydrogen atoms were included in the refinement. The thermal displacement parameters were refined anisotropically for non-hydrogen atoms and isotropically for hydrogen atoms. Full-matrix least-squares methods were applied using all of the unique reflection data. Crystal data are summarized in Table 1 and selected structural parameters in Tables 2 and 3.

Magnetic Measurements. dc magnetic susceptibilities of randomly oriented polycrystalline samples of 4ImNNH and **1**−**12** were measured on a Quantum Design MPMS SQUID magnetometer equipped with a 7 T coil in a temperature range 1.8−300 K. The magnetic responses were corrected with diamagnetic blank data of the sample holder measured separately. The diamagnetic contribution of the sample itself was estimated from Pascal's constants.

Results

Characterization of 4ImNNH. The molecular structure of 4ImNNH was determined by X-ray crystallographic analysis (see Supporting Information, Figure S1). Since the hydrogen atoms could be found experimentally, we determined the exact form of 4ImNNH because the imidazole ring in 4ImNNH possesses tautomeric isomerism. The 4ImNNH molecule was proved to possess a 1*H*-form in the crystal, as indicated by imino N1 and amino N2 nitrogen atoms in Figure 1. In contrast to our expectation, the imidazole N−H proton does not form an intramolecular chelate. Instead, it participates in a branching H-bond in an

(9) Omata, J.; Ishida, T.; Hashizume, D.; Iwasaki, F.; Nogami, T. *Inorg. Chem.* **2001**, *40*, 3954. Omata, J.; Ishida, T.; Hashizume, D.; Iwasaki, F.; Nogami, T. *Mol. Cryst. Liq. Cryst.* **2002**, *376*, 455.
(10) Fegy, K.; Luneau, D.; Ohm, T.; Paulsen, C.; Rey, P. *Angew. Chem., Int. Ed.* **1998**, *37*, 1270. Fegy, K.; Sanz, N.; Luneau, D.; Belorizky, E.; Rey, P. *Inorg. Chem.* **1998**, *37*, 4518. Fegy, K.; Luneau, D.; Belorizky, E.; Novac, M.; Tholence, J.-L.; Paulsen, C.; Ohm, T.; Rey, P. *Inorg. Chem.* **1998**, *37*, 4524.
(11) Aoki, C.; Ishida, T.; Nogami, T. *Inorg. Chem. Commun.* **2003**, *6*, 1122.
(12) Miller, J. S.; Epstein, A. J.; Reiff, W. M. *Acc. Chem. Res.* **1988**, *21*, 114.
(13) Ullman, E. F.; Osiecki, J. H.; Boocock, D. G. B.; Darcy, R. *J. Am. Chem. Soc.* **1972**, *94*, 7049.
(14) Altomare, A.; Burla, M. C.; Camalli, M.; Cascarano, G.; Giacovazzo, C.; Guagliardi, A.; Moliterni, A. G. G.; Polidori, G.; Spagna, R. *J. Appl. Crystallogr.* **1999**, *32*, 115.
(15) TeXsan, Single-Crystal Structure Analysis Software, ver. 1.10, Molecular Structure Corp., The Woodlands, TX, and Rigaku Co. Ltd., Akishima, Tokyo, Japan, 1999.

Table 1. Crystallographic Data for 4ImNNH, $[M(4ImNNH)_2(NO_3)_2]$ (M = Mn (**1**), Co (**2**), Ni (**3**), Cu (**4**)), $[Mn(4ImNNH)_2Cl_2]$ (**5**), and $[Cu(4ImNNH)_2Br_2]$ (**12**)

compds	4ImNNH	**1**	**2**	**3**	**4**	**5**	**12**
formula	$C_{10}H_{15}N_4O_2$	$C_{20}H_{30}N_{10}O_{10}Mn_1$	$C_{20}H_{30}N_{10}O_{10}Co_1$	$C_{20}H_{30}N_{10}O_{10}Ni_1$	$C_{20}H_{30}N_{10}O_{10}Cu_1$	$C_{20}H_{30}Cl_2N_8O_4Mn_1$	$C_{20}H_{30}Br_2N_8O_4Cu_1$
habit	black platelet	black block	black block	black block	black block	black platelet	black platelet
dimension (mm^3)	0.5 × 0.5 × 0.1	0.8 × 0.5 × 0.2	0.4 × 0.2 × 0.1	0.3 × 0.3 × 0.1	0.4 × 0.35 × 0.08	0.3 × 0.3 × 0.08	0.4 × 0.3 × 0.08
T/K	90	100	100	100	100	100	100
cryst syst	tetragonal	monoclinic	monoclinic	monoclinic	monoclinic	triclinic	monoclinic
space group	$I4_1/a$	$P2_1/a$	$P2_1/a$	$P2_1/a$	$P2_1/a$	$P\bar{1}$	$P2/c$
a (Å)	20.7966(9)	13.3749(9)	13.3545(2)	13.3490(9)	12.7794(7)	7.5167(9)	17.603(2)
b (Å)	20.7966(9)	11.0529(9)	10.8843(3)	10.9253(7)	11.1557(7)	8.917(1)	7.4777(7)
c (Å)	10.6931(5)	13.3455(7)	13.3566(5)	13.297(1)	13.191(1)	9.743(2)	17.582(2)
α (deg)	90	90	90	90	90	76.161(4)	90
β (deg)	90	43.615(2)	43.306(1)	43.384(2)	44.373(2)	85.579(3)	35.096(4)
α (deg)	90	90	90	90	90	87.805(5)	90
V ($Å^3$)	4624.7(3)	1360.9(2)	1331.62(7)	1332.1(2)	1315.2(2)	632.1(1)	1330.6(3)
Z	16	2	2	2	2	1	2
D_{calc} ($g\ cm^{-3}$)	1.282	1.526	1.570	1.569	1.601	1.503	1.672
unique data for refinement	2656	3087	3032	2815	2803	2487	2893
μ (Mo Kα) (mm^{-1})	0.093	0.557	0.718	0.802	0.905	0.777	3.874
$R(F)^a$ ($I > 2\sigma(I)$)	0.0402	0.0546	0.0671	0.0624	0.0633	0.0531	0.0673
$R_w(F^2)^b$ (all data)	0.0874	0.1388	0.1797	0.1659	0.2061	0.1466	0.1913

[a] $R = \sum||F_o| - |F_c||/\sum|F_o|$. [b] $R_w = [\sum w(F_o^2 - F_c^2)^2/\sum w(F_o^2)^2]^{1/2}$.

Table 2. Selected Bond Lengths (Å), Bond Angles (deg), and Dihedral Angles (deg) for $[M(4ImNNH)_2(NO_3)_2]$ (M = Mn (**1**), Co (**2**), Ni (**3**), Cu (**4**))

M	Mn	Co	Ni	Cu
M1−O1	2.132(1)	2.035(2)	2.038(2)	1.986(3)
M1−N1	2.167(2)	2.063(3)	2.020(3)	1.948(3)
M1−O3	2.240(1)	2.159(2)	2.129(2)	2.473(2)
O1−N3	1.293(2)	1.304(3)	1.302(3)	1.302(4)
O2−N4	1.276(2)	1.273(3)	1.271(4)	1.278(4)
N1−C2	1.389(3)	1.393(4)	1.384(4)	1.396(4)
N3−C4	1.350(3)	1.328(4)	1.331(4)	1.328(5)
N4−C4	1.355(3)	1.358(4)	1.361(4)	1.351(4)
C2−C4	1.438(3)	1.437(4)	1.436(5)	1.438(5)
O1−M1−O3	94.77(5)	94.04(7)	95.37(9)	92.50(9)
O1−M1−N1	85.11(6)	89.26(9)	89.4(1)	88.1(1)
O3−M1−N1	88.15(6)	87.38(8)	89.4(1)	90.0(1)
M1−O1−N3	127.8(1)	126.1(2)	125.6(2)	124.7(2)
M1−O3−N5	120.4(1)	121.9(2)	123.8(2)	115.2(2)
M1−N1−C2	126.9(1)	126.1(2)	126.4(2)	126.7(3)
O3−M1−O1−N3	68.6(1)	72.7(2)	83.2(2)	77.1(2)
O3−M1−N1−C2	−84.3(1)	−87.4(2)	−93.6(2)	−88.5(2)
M1−O1−N3−C4	18.6(2)	15.7(3)	6.3(4)	15.6(4)
M1−N1−C2−C4	−1.3(2)	1.1(3)	3.0(4)	3.6(4)
N1−C2−C4−N3	−7.3(3)	−5.8(4)	−5.5(5)	−5.7(5)

intermolecular manner; the intermolecular $H3_{ImH}\cdots O1_{NN}'$ and $H3_{ImH}\cdots N1_{ImH}'$ distances are 2.24(1) and 2.06(1) Å, respectively, which are much shorter than the sum of the van der Waals radii (2.7 Å),[16] where the symmetry operation code for ′ is $^3/_4 - y$, $-^3/_4 + x$, $^1/_4 + z$. This finding suggests the potential ability of acidic H3 to form H-bonds when 4ImNNH is incorporated in coordination compounds. The strongly directive nature of the branching H-bond near a right angle leads to a 4_1 helix structure in an $I4_1/a$ space group. The purity of 4ImNNH was confirmed by the Curie−Weiss analysis ($\chi_{mol} = C/(T - \theta)$) of the magnetic susceptibility, giving $C = 0.370\ cm^3\ K\ mol^{-1}$ ($0.375\ cm^3\ K\ mol^{-1}$ in theory) with $\theta = -0.52$ K.

(16) Bondi, A. *J. Phys. Chem.* **1964**, *68*, 441.

Table 3. Intermolecular Atomic Distances (Å) for $[M(4ImNNH)_2(NO_3)_2]$ (M = Mn (**1**), Co (**2**), Ni (**3**), Cu (**4**))[a]

M	Mn	Co	Ni	Cu
C1···O2#	2.986(3)	2.948(4)	2.939(4)	2.948(5)
N2···O2#	3.382(3)	3.291(3)	3.245(4)	3.281(4)
H1···O2#	2.38(2)	2.41(3)	2.36(4)	2.45(5)
H3···O2#	3.15(3)	3.13(4)	3.32(9)	3.12(5)
O3···C3#	3.287(3)	3.311(4)	3.239(4)	3.186(5)
O3···N2#	3.093(3)	3.146(4)	3.103(4)	3.067(4)
O3···H2#	2.85(3)	2.86(4)	2.72(4)	2.58(4)
O3···H3#	2.54(3)	2.49(4)	2.15(9)	2.45(5)
O4···N2#	2.823(2)	2.797(3)	2.801(4)	2.741(4)
O4···H3#	2.00(3)	1.93(4)	1.67(8)	1.68(6)

[a] Symmetry operation code for # is $^3/_2 - x$, $-^1/_2 + y$, $-z + 1$.

X-ray Crystal Structure Analysis of $[M(4ImNNH)_2X_2]$. Table 1 shows the cell parameters of **1**−**4**. Their crystal structures are practically identical, belonging to a monoclinic space group $P2_1/a$. Figure 2a shows the molecular structure of **1** (for those of **2**−**4**, see Figure S2, Supporting Information). Half of the molecule is crystallographically independent; the octahedral M ion resides at an inversion center. The metal ion is coordinated by two NN oxygen atoms and two imidazole nitrogen atoms from the equatorial positions. The axial positions are occupied by nitrate oxygen atoms. Table 2 summarizes the selected bond lengths and angles. The octahedrons are elongated by ca. 0.1 Å for **1**−**3** and 0.5 Å for **4**. The axial directions are slightly deviated from the normal of the equatorial plane, as indicated by the O1−M1−O3 and O3−M1−N1 angles ranging from 94.04(7) to 95.37(9)° and 87.38(8) to 89.4(1)°, respectively,

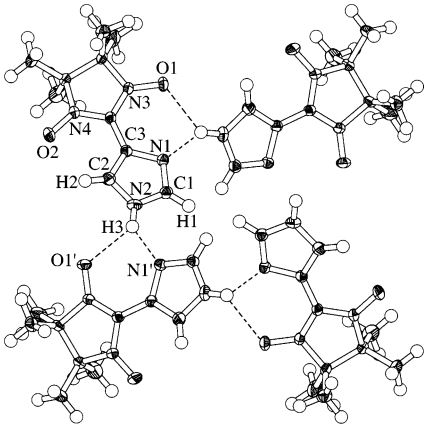

Figure 1. Ortep drawing of four 4ImNNH molecules at the 50% probability level. They form a 4_1 helix along the *c* axis. Intermolecular hydrogen bonds are indicated with dotted lines. The distances are 2.24(1) Å for $H3_{ImH}\cdots O1_{NN}'$ and 2.06(1) Å for $H3_{ImH}\cdots N1_{ImH}'$. The symmetry operation code for ′ is $^3/_4 - y$, $-^3/_4 + x$, $^1/_4 + z$.

for **1**−**3**. For **4**, these angles were nearly orthogonal (92.50(9) and 90.0(1)°, respectively).

The six-membered chelate rings are slightly deviated from an ideal plane, as indicated by the torsion angle around M1−O1−N3−C4, M1−N1−C2−C4, and N1−C2−C4−N3. Interestingly, the torsion angle around M1−O1−N3−C4 drastically decreases in the order of Mn, Co, and Ni, which seems to be related to the bond lengths of M−O and M−N and also to the deformation from an ideal octahedron. The shorter bond lengths bring about smaller and less distorted six-membered rings, and accordingly the chelate ring in **3** is highly planar with negligible torsion. On the other hand, the torsion angle around M1−O1−N3−C4 in **4** is much larger than that in **3**. The steric congestion of the chelate ring may increase possibly because of too short equatorial M−O and M−N bonds. The torsion around M1−O1−N3−C4 is most important for magnetic coupling between the M spin and the NN radical spin, especially for M = Ni and Cu, from the viewpoint of the overlap between two magnetic orbitals (see below).

Intermolecular H-bonds are found in the crystals of **1**−**4**. Figure 2b shows the molecular arrangement of **1**. The NH group in the imidazole ring plays a key role: this hydrogen atom (H3) is located considerably close to nitrate oxygen atoms in a neighboring molecule as indicated by d_1 ($O4_{nitrate}\cdots H3_{ImH}$#) and d_2 ($O3_{nitrate}\cdots H3_{ImH}$#) in Figure 2b and also slightly close to a nitroxide oxygen atom with the $H3_{ImH}\cdots O2_{NN}$# distance of 3.15(3) Å (the symmetry operation code for # is $^3/_2 - x$, $y - {}^1/_2$, $-z + 1$). In the latter geometry a very short C−H···O contact is also found between H1 and $O2_{NN}$# (d_3 in Figure 2b), which is shorter than the sum of the van der Waals radii (2.7 Å).[16] As Figure 2b shows, there are two strands between the H-donor/acceptor and H-acceptor/donor sites in each neighboring pair. This geometry successively repeats along the $a + b$ and $a - b$ directions, owing to the symmetry, and accordingly they form a two-dimensional H-bond network parallel to the *ab* plane (Figure 2c). A detailed description on the structure of **3** has been reported elsewhere.[11] The multiple and self-

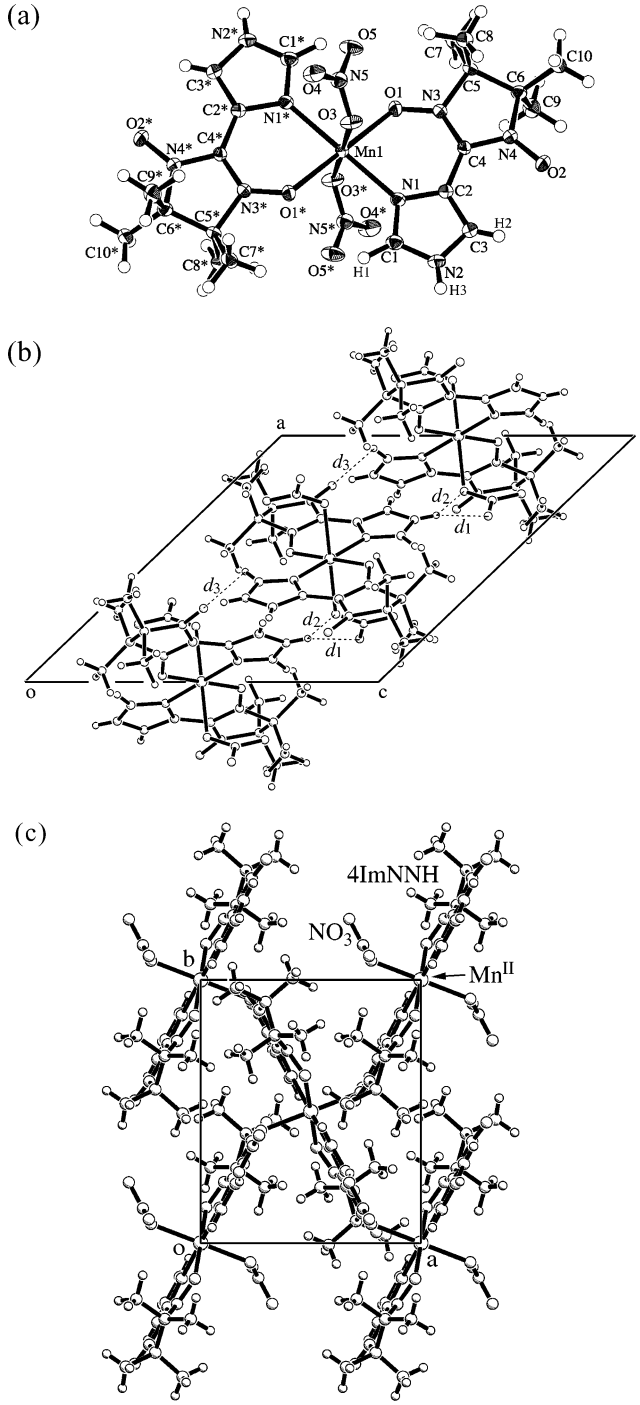

Figure 2. (a) Ortep drawing of the molecular structure of [Mn(4ImNNH)$_2$(NO$_3$)$_2$] (**1**) at the 50% probability level. Atomic numbering is also shown. The symmetry operation code for * is $1 - x$, $1 - y$, $1 - z$. (b) Molecular arrangement in the crystal of **1** viewed along the *b* axis. Intermolecular hydrogen bonds are indicated with dotted lines. The distances are as follows: d_1($O4_{nitrate}\cdots H3_{ImH}$#) = 2.00(3) Å; d_2($O3_{nitrate}\cdots H3_{ImH}$#) = 2.54(3) Å; d_3($H1_{ImH}\cdots O2_{NN}$#) = 2.38(2) Å, where the symmetry operation code for # is $^3/_2 - x$, $-{}^1/_2 + y$, $1 - z$. (c) Molecular arrangement in the crystal of **1** viewed along the *c* axis.

complementary H-bonds stabilize the side-by-side molecular arrangement,[17] and therefore **1**−**4** are assumed to afford isomorphous crystals. The interatomic distances are summarized in Table 3.

(17) For example, Zeng, H.; Yang, X.; Brown, A. L.; Martinovic, S.; Smith, R. D.; Gong, B. *Chem. Commun.* **2003**, 1556.

Table 4. Selected Bond Lengths (Å), Bond Angles (deg), and Dihedral Angles (deg) for $[Mn(4ImNNH)_2Cl_2]$ (**5**) and $[Cu(4ImNNH)_2Br_2]$ (**12**)

compound	**5** (M = Mn, X = Cl)	**12** (M = Cu, X = Br)
M1−O1	2.168(2)	2.032(3)
M1−N1	2.193(2)	1.934(4)
M1−X1	2.5425(6)	3.0058(5)
O1−N3	1.300(3)	1.302(5)
O2−N4	1.281(3)	1.275(6)
N1−C2	1.314(4)	1.376(6)
N3−C4	1.343(4)	1.336(7)
N4−C4	1.355(4)	1.344(6)
C2−C4	1.428(4)	1.426(6)
O1−M1−X1	92.46(5)	96.98(9)
O1−M1−N1	82.81(8)	89.7(2)
X1−M1−N1	89.50(6)	88.67(9)
M1−O1−N3	118.0(2)	119.4(3)
M1−N1−C2	123.1(2)	124.2(3)
X1−M1−O1−N3	136.0(2)	127.2(3)
X1−M1−N1−C2	−123.9(2)	−122.0(4)
M1−O1−N3−C4	−44.2(3)	−34.4(6)
M1−N1−C2−C4	9.4(3)	5.7(6)
N1−C2−C4−N3	14.6(4)	13.0(7)

We also prepared $[M(4ImNNH)_2X_2]$ complexes from metal chlorides and bromides to search for ferromagnetic systems. Elemental analysis clarified the stoicheometry of all of the complexes as $[M(4ImNNH)_2X_2]$. Only two of them could afford good crystals suitable for X-ray crystallographic analysis. The molecular structures of $[Mn(4ImNNH)_2Cl_2]$ (**5**) (Figure S3a, Supporting Information) is similar to those of **1**−**4** except for the axial ligands; the metal ion resides at the crystal inversion center and two 4ImNNH ligands occupy at the equatorial positions. Selected geometrical parameters are listed in Table 4. Although **1** and **5** possess different molecular packing, as indicated by the crystal systems and space groups ($P2_1/a$ and $P\bar{1}$ for **1** and **5**, respectively), intermolecular H-bonding is also formed in $Cl1\cdots H3_{ImH}{}^{\dagger}$ for **5** (Figure 3a), like $H_{ImH}\cdots O_{nitrate}$ in **1**. The $Cl1\cdots H3_{ImH}{}^{\dagger}$ distance was 2.16(4) Å, which is much shorter than the sum of the van der Waals radii (2.95 Å).[16] The nearest neighboring molecules of **5** are related by the *a*-axis translation and connected with two H-bonds of a H-donor/acceptor and H-acceptor/donor pair. The double H···Cl H-bonds successively repeat along the *a* axis, thus constructing a H-bonding ladder structure.

X-ray crystal structure analysis on $[Cu(4ImNNH)_2Br_2]$ (**12**) was also successful. The molecular structure of **12** (Figure S3, Supporting Information) is similar to that of **5** expected for the axial ligand. Owing to the elongated distortion from an octahedron and to the large covalent radius of Br, the Cu−Br bond length of 3.0058(5) Å is extremely long (Table 4), leading to a different molecular packing and space group ($P2/c$) compared with **5** and the nitrate compounds. The important torsion angle around M1−O1−N3−C4 in **12** is much larger than those in **3** and **4**. Despite the different space group, a similar intermolecular H-bond could also be found in the crystal of **12** (Figure 3b). The $Br1\cdots H3_{ImH}{}^{\ddagger}$ distance (2.41(6) Å) is much shorter than the sum of the van der Waals radii (3.05 Å).[16] The nearest neighboring molecules of **12** are related to the *b*-axis translation. The H···Br H-bonds repeat along the *b* axis, giving a H-bond ladder structure like **5**.

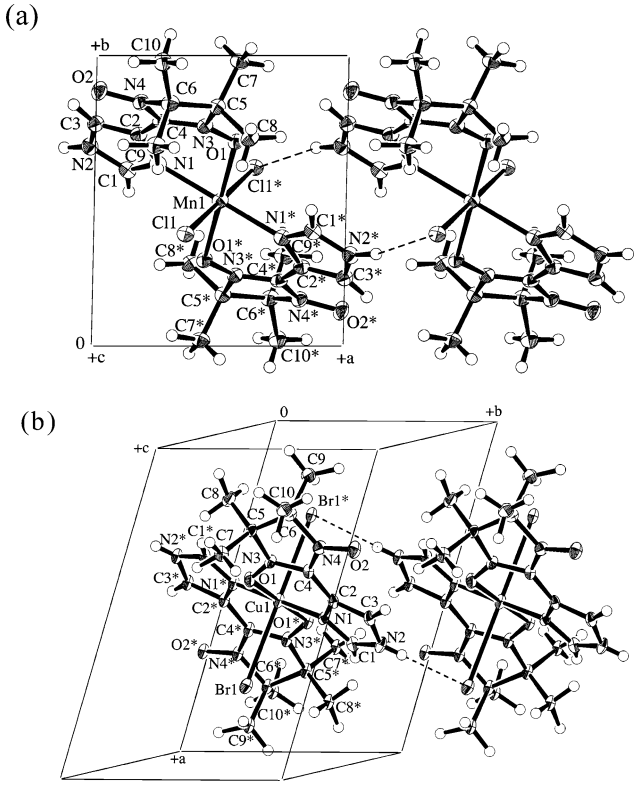

Figure 3. (a) Molecular arrangement in the crystals of **5** viewed along the *c* axis. Intermolecular hydrogen bonds are indicated with dotted lines. The distance is $d(Cl1\cdots H3_{ImH}{}^{\dagger}) = 2.16(4)$ Å. The symmetry operation codes for * and † are $1-x, 1-y, 1-z$ and $-1+x, y, z$, respectively. (b) Molecular arrangement in the crystals of **12**. Intermolecular hydrogen bonds are indicated with dotted lines. The distance is $d(Br1\cdots H3_{ImH}{}^{\ddagger}) = 2.41(5)$ Å. The symmetry operation codes for * and ‡ are $1-x, 1-y, 1-z$ and $x, 1+y, z$, respectively.

The cystal structures determined here on the $[M(4ImNNH)_2X_2]$-type complexes always have the intermolecular H-bonds of H(imidazole)···X(axial ligand)−M, regardless of the various space groups. The two-dimensional networks are found in the nitrate complexes (**1**−**4**) and the one-dimensional ladder in the halide complexes (**5** and **12**).

Magnetic Properties of $[M(4ImNNH)_2X_2]$. Figure 4a shows the temperature dependence of the $\chi_{mol}T$ values for **1**−**4** measured at 5 kOe. The $\chi_{mol}T$ value of **1** decreases with decreasing temperature down to ca. 20 K, indicating the presence of antiferromagnetic coupling. The observed $\chi_{mol}T$ value of 3.16 cm^3 K mol^{-1} at 300 K is much smaller than the theoretical spin-only value of 5.1 cm^3 K mol^{-1}. The plateau around 30 K has 1.80 cm^3 K mol^{-1}, which corresponds to the spin-only value 1.88 cm^3 K mol^{-1} with $S_{total} = {}^3/_2$. Thus, the decrease of $\chi_{mol}T$ can be ascribed to considerably strong intramolecular antiferromagnetic (ferrimagnetic) coupling through the direct manganese−radical bonds. Below 20 K, the $\chi_{mol}T$ value of **1** turns to increase on cooling. This behavior is ascribed to intermolecular ferromagnetic interaction.

The $\chi_{mol}T$ value for **2** behaves similar to that of **1**. With decreasing temperature the $\chi_{mol}T$ value of **2** once decreases and increases very slightly below 4 K, indicating intermolecular ferromagnetic coupling among the ferrimagnetically correlated radical−cobat(II)−radical molecules with $S_{total} =$

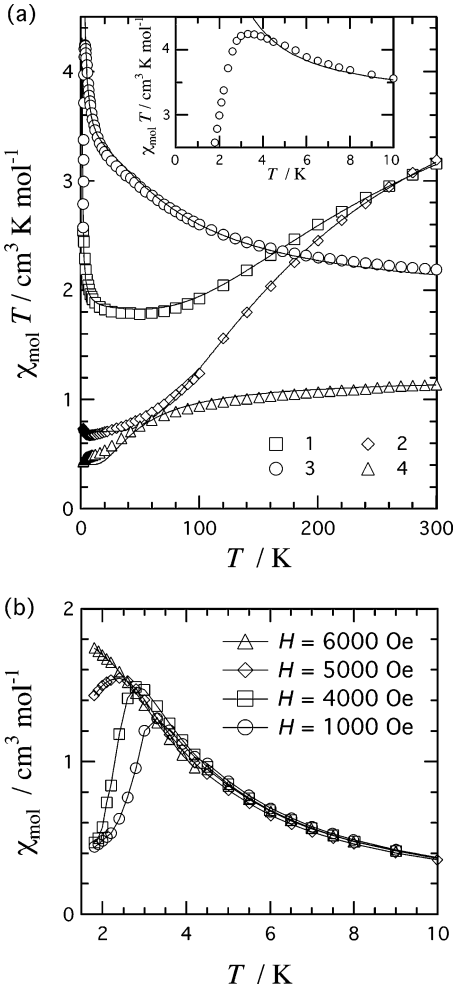

Figure 4. (a) Temperature dependence of the $\chi_{mol}T$ values for [M(4ImNNH)$_2$(NO$_3$)$_2$] (M = Mn (**1**), Co (**2**), Ni (**3**), Cu(**4**)) measured at 5 kOe. Solid lines represent the calculated values. For the equations and parameters, see the text and Table 5. Inset: magnification of a low-temperature region for **3**. (b) Temperature dependence of χ_{mol} (or M/H in an ordered state) for **3** measured at 1, 4, 5, and 6 kOe. Solid lines are shown for a guide to the eye.

$^1/_2$. We have to take into account the contribution of angular momentum for the cobalt(II) complex and the van Vleck treatment may give only approximate results, while manganese(II), nickel(II), and copper(II) ions usually have negligible contribution of angular momentum. However, the optimized result well-reproduced the experimental data (the solid lines in Figure 4a), which supports the belief that the temperature dependence of the $\chi_{mol}T$ value is reasonably ascribed mainly to the magnetic exchange coupling. The $\chi_{mol}T$ value for **4** shows monotonic decrease, suggesting that intramolecular magnetic coupling is antiferromagnetic. The $\chi_{mol}T$ value around 10 K agrees with $S_{total} = {}^1/_2$.

On the other hand, the $\chi_{mol}T$ value of **3** increases with decreasing temperature. The observed $\chi_{mol}T$ value around a bend at 14 K is 3.3 cm^3 K mol^{-1}, which is slightly larger than the spin-only value 3.0 cm^3 K mol^{-1} for $S_{total} = 2$. The secondary sharp increase below 14 K is due to intermolecular ferromagnetic interaction. Therefore, both intra- and intermolecular magnetic couplings are ferromagnetic. An abrupt drop was observed at 4 K, suggesting that magnetic phase transition takes place near the peaking temperature. We measured the field dependence of the peaking behavior of **3** (Figure 4b). The χ_{mol} peaks were found at 3.3, 2.8, and 2.4 K when the external fields of 1, 4, and 5 kOe were applied, respectively, and finally the peak vanished at 6 kOe. This finding suggests that the ground state of **3** is antiferromagnetic, despite the presence of both ferromagnetic intra- and intermolecular interactions.

The molecular structures of **1**−**4** are regarded as a linear radical−metal−radical triad system, and the $\chi_{mol}T$ values are quantitatively analyzed according to the spin exchange Hamiltonian $H = -2J(S_1 \cdot S_2 + S_2 \cdot S_3)$ based on the molecular symmetry; the suffixes 1 and 3 denote NN and 2 denotes metal spins. The van Vleck treatment gave the following expressions (eqs 1−4)[18] for **1**−**4**, respectively. The Weiss temperature is introduced for intermolecular magnetic interaction. The optimized parameters are summarized in Table 5. The calculated curves are superposed on the data points in Figure 4a, and the fittings are satisfactory. This fact supports the reliability of the spin−spin coupling model, although there is possibility of the presence of zero-field splitting or other origins of single ions for **1**−**3**.

$$\chi_{mol} = \frac{N_A g^2 \mu_B}{4k(T-\theta)} \frac{10\exp(-7J/kT) + 35\exp(-2J/kT) + 35 + 84\exp(5J/kT)}{2\exp(-7J/kT) + 3\exp(-2J/kT) + 3 + 4\exp(5J/kT)} \quad (1)$$

$$\chi_{mol} = \frac{N_A g^2 \mu_B}{4k(T-\theta)} \frac{\exp(-5J/kT) + 10\exp(-2J/kT) + 10 + 35\exp(3J/kT)}{\exp(-5J/kT) + 2\exp(-2J/kT) + 2 + 3\exp(3J/kT)} \quad (2)$$

$$\chi_{mol} = \frac{2N_A g^2 \mu_B}{k(T-\theta)} \frac{\exp(-2J/kT) + 1 + 5\exp(2J/kT)}{\exp(-4J/kT) + 3\exp(-2J/kT) + 3 + 5\exp(2J/kT)} \quad (3)$$

$$\chi_{mol} = \frac{N_A g^2 \mu_B}{2k(T-\theta)} \frac{\exp(-2J/kT) + 1 + 10\exp(J/kT)}{2\exp(-2J/kT) + 2 + 4\exp(J/kT)} \quad (4)$$

The intermolecular ferromagnetic interaction was finally confirmed by the $M-H$ curves (magnetization curves as a function of applied magnetic field). Figure 5 shows the $M-H$ curves of **1** measured at 1.8 and 3.5 K. The observed magnetization at 3.5 K rapidly increased over the theoretical Brillouin function of $S_{total} = {}^3/_2$ and the saturation was more significant at 1.8 K, clearly indicating the presence of intermolecular ferromagnetic interaction. Unfortunately, compound **1** did not undergo any magnetic phase transition down to 1.8 K. Note that the saturation magnetization of 1.52×10^4 erg Oe^{-1} mol^{-1} at 70 kOe corresponds to the antiferromagnetically correlated radical−metal−radical system of $S_{total} = {}^3/_2$, in sharp contrast to that of **3** owing to the intramolecular ferromagnetic correlation (see below).

(18) Gruber, S. J.; Harris, C. M.; Sinn, E. *J. Chem. Phys.* **1968**, *49*, 2183.

Table 5. Optimized Parameters g, J/k_B, and θ of $[M(4ImNNH)_2X_2]$ (M = Mn, Co, Ni, Cu; X = NO_3, Cl, Br)[a]

X	M	g	$2Jk_B^{-1}$/K	θ/K
NO_3	Mn (**1**)	1.96(1)	−140(3)	0.58(2)
	Co (**2**)	2.75(1)	−155(2)	0[b,c]
	Ni (**3**)	2.06(1)	85(3)	1.04(3)
	Cu (**4**)	2.08(1)	−58(4)	0[b]
Cl	Mn (**5**)	2.01(1)	−175(2)	0.52(1)
	Co (**6**)	2.69(2)	−270(4)	0.11(6)
	Ni (**7**)	2.22(1)	−201(2)	0[b]
	Cu (**8**)	2.11(1)	−247(7)	−2.7(2)
Br	Mn (**9**)	1.95(1)	−156(2)	0.24(1)
	Co (**10**)	2.57(1)	−238(2)	0[b]
	Ni (**11**)	2.28(4)	−165(2)	0[b]
	Cu (**12**)	2.05(1)	−372(5)	1.69(7)

[a] The Heisenberg spin Hamiltonian is defined as $H = -2J(S_1 \cdot S_2 + S_2 \cdot S_3)$. [b] The Weiss temperature is not included in the parameter optimization. [c] A very small positive θ is assumed.

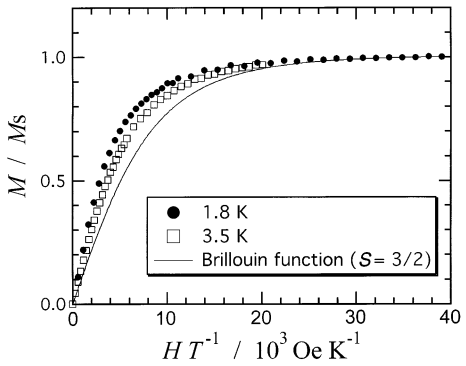

Figure 5. $M-H$ curves of $[Mn(4ImNNH)_2(NO_3)_2]$ (**1**) measured at 1.8 and 3.5 K. A solid line represents the theoretical Brillouin function of $S = {}^3/_2$.

To elucidate the magnetic ground state of **3**, we measured the $M-H$ curve of **3** at 1.8 K. As Figure 6a shows, the ground state is antiferromagnetic and a metamagnetic transition occurs near 5.5 kOe with a very small hysteresis during the metamagnetic transition. The critical field determined here is consistent with the disappearance of the χ_{mol} peak on applying the field as shown in Figure 4b. The metamagnetism implies the simultaneous presence of intermolecular ferro- and antiferromagnetic interactions. The temperature dependence of χ_{mol} for **3** reveals two main ferromagnetic exchange couplings ascribable to intra- and intermolecular interactions. This finding indicates that an additional weak antiferromagnetic interaction is operative in the crystal of **3**. The saturation magnetization was ca. 2.0×10^4 erg Oe^{-1} mol^{-1}, in good agreement with the ground $S_{total} = 2$ species where all spins are ferromagnetically correlated. The transition temperature (T_N) was determined by means of the field-cooled magnetization measurements at 5 Oe (Figure 6b). A sharp peak was found at 3.4 K, which we define as the magnetic phase transition temperature.

The magnetic susceptibilities of **5**−**12** were measured (Figure 7) and analyzed using eqs 1−4. The optimized parameters are summarized in Table 5, which clearly shows that all of them exhibited intramolecular antiferomagnetic coupling and that four complexes (**5**, **6**, **9**, and **12**) exhibited intermolecular ferromagnetic coupling. The calculated curves reproduce well the experimental data, supporting the proposed molecular structure of radical−metal−radical systems.

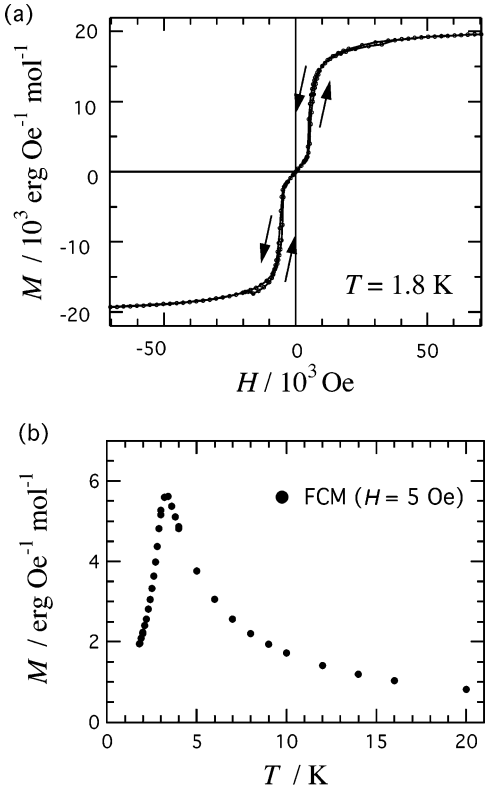

Figure 6. (a) $M-H$ curve of $[Ni(4ImNNH)_2(NO_3)_2]$ (**3**) measured at 1.8 K. Solid lines are drawn for a guide to the eye. (b) Field-cooled magnetization of **3** measured at 5 Oe.

Their field-cooled magnetization measurements revealed that they underwent no magnetic phase transition above 1.8 K.

Discussion

Intramolecular Ferromagnetic Coupling. The electron configurations of the high-spin Mn^{II} and Co^{II} ions are $(t_{2g})^3(e_g)^2$ and $(t_{2g})^5(e_g)^2$, respectively, and therefore the intramolecular antiferromagnetic couplings between the magnetic t_{2g} spins and the nitroxide π^* spin are explained in terms of the $d\pi-p\pi$ orbital overlap, which dominantly contributes to the total magnetic interaction observed, compared with minor $d\sigma-p\pi$ contribution. On the other hand, Ni^{II} and Cu^{II} ions have only e_g spins, that is, $d\sigma$ spins, and the magnetic coupling may be ferromagnetic depending largely on the coordination geometry.

When TEMPO and PROXYL radicals are available, the magnetic interactions between copper(II) and equatorially coordinated nitroxide radicals are usually observed to be antiferromagnetic[19] (TEMPO = 2,2,6,6-tetramethylpiperidin-1-yloxyl, PROXYL = 2,2,4,4-tetramethylpyrrolidin-1-yloxyl). However, Luneau and co-workers reported pioneering works on the ferromagnetic interaction between metal and radical spins in $[M(hfac)_2(2PyIN)]$ (M = Ni, Cu; hfac = 1,1,1,5,5,5-hexafluoropentane-2,4-dionate) where IN denotes the imino nitroxide radical (Chart 2).[20] It has been established that the ferromagnetic coupling is caused by the strict

(19) Dickman, M. H.; Doedens, R. J. *Inorg. Chem.* **1981**, *20*, 2677. Porter, L. C.; Dickmann, M. H.; Doedens, R. J. *Inorg. Chem.* **1983**, *22*, 1962. Porter, L. C.; Doedens, R. J. *Inorg. Chem.* **1985**, *24*, 1006. Lim, Y. Y.; Drago, R. S. *Inorg. Chem.* **1972**, *11*, 1334.

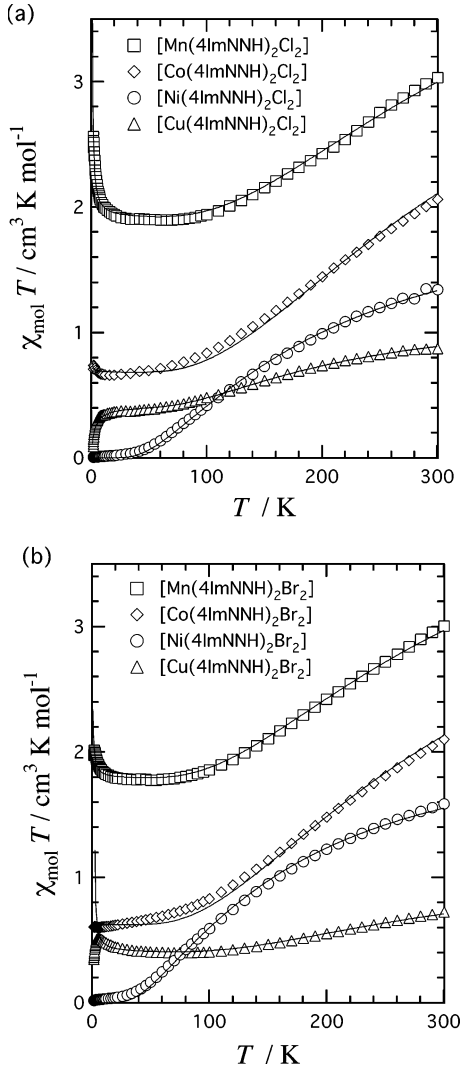

Figure 7. Temperature dependence of the $\chi_{mol}T$ values for $[M(4ImNNH)_2X_2]$ (M = Mn, Co, Ni, Cu; X = Cl (a), Br (b)) measured at 5 kOe. Solid lines represent the calculated values. For the equations and parameters, see the text and Table 5.

Chart 2

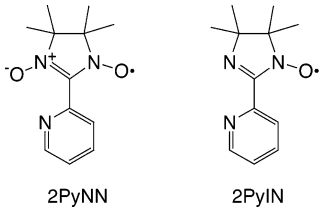

orthogonality between the metal dσ and radical π* spins as described in Figure 8a when radical chelate ligands, such as 2PyIN[20] and *o*-semiquinones,[21] are coordinated at the equatorial positions. Kaizaki and co-workers also supported the above mechanism from the study on $[NiCl_2(2PyIN)_2]$.[22] The highly planar five-membered chelate ring plays a very important role in the ferromagnetic interactions. On the other hand, in the case of the corresponding 2PyNN derivative, the intramolecular coupling in $[Cu(ClO_4)_2(2PyNN)]$ was antiferromagnetic.[23] The reason arises from a severe nonplanar distortion[24] to lose the orthogonality (Figure 8b) like the TEMPO and PROXYL cases.[19] Therefore, in contrast to the literature results, **3** having six-membered chelate rings showed exceptionally intramolecular ferromagnetic interaction. As the X-ray diffraction study of **3** reveals, the chelate ring is highly planar, owing to the advantage of the imidazole ring used. Namely, the imidazole ring is less bulky than the pyridine ring so that the bent chelate structure can be spread to recover a plane.

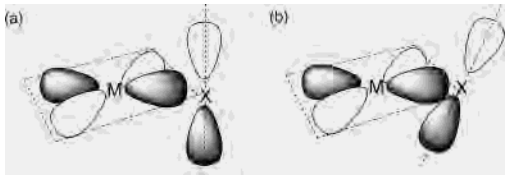

Figure 8. Schematic drawings of mutual geometries between magnetic dσ(metal) and pπ*(O in nitronyl nitroxide, N in imino nitroxide) orbitals for nickel(II) and copper(II) complexes coordinated by nitronyl nitoxide or imino nitroxide from equatorial positions. (a) A strictly orthogonal case. (b) An overlapped case.

The considerably large ferromagnetic interactions were found in the semiquinone complexes containing copper(II) ($2J/hc = 220$ cm^{-1}) and nickel(II) ($2J/hc > 400$ cm^{-1}).[21] In the 2PyIN complexes, fairly large ferromagnetic interactions were observed as well; $2J/hc > 300$ cm^{-1} for the copper(II) complex and 94 cm^{-1} for the nickel(II) one.[7] The magnetic couplings due to the direct equatorial coordination of the radical center are usually very large, but the present value of **3** is only moderate (85(3) K corresponds to 60(2) cm^{-1}). Antiferromagnetic contribution due to orbital overlap seems to cancel out partly the large ferromagnetic coupling. In view of the fact that there has been found only one case showing intramolecular ferromagnetic interaction among six dσ complexes $[M(4ImNNH)_2X_2]$ (M = Ni, Cu; X = NO_3, Cl, Br), the present dσ complexes seem to lie on the border between the orthogonal and overlapped cases (Figure 8) in connection with nonplanar distortion of the chlate rings.

Complexes **4** and **12** having copper ions showed intramolecular antiferromagnetic interactions and the magnitude of the magnetic coupling in **12** ($2J/k_B = -372(5)$ K) is much larger than that of **4** (−58(4) K; Table 5). The antiferromagnetic contribution is supposed to increase with an increase of the M1−O1−N3−C4 torsion angle. The larger Cu1−O1−N3−C4 torsion (−34.4(6)°) in **12** is responsible for the larger negative *J* value in comparison with the case of **4** (Tables 2 and 4).

Intermolecular Ferromagnetic Coupling. We have clearly demonstrated that **3** is a metamagnet below 3.4 K. The measurements of temperature dependence of χ_{mol} revealed

(20) Luneau, D.; Rey, P.; Laugier, J.; Fries, P.; Caneschi, A.; Gatteschi, D.; Sessoli, R. *J. Am. Chem. Soc.* **1991**, *113*, 1245. Luneau, D.; Rey, P.; Laugier, J.; Belorizky, E.; Conge, A. *Inorg. Chem.* **1992**, *31*, 3578.
(21) Kahn, O.; Prins, R.; Reedijk, J.; Thompson, J. S. *Inorg. Chem.* **1987**, *26*, 3557. Benelli, C.; Dei. A.; Gatteschi, D.; Pardi, L. *Inorg. Chem.* **1988**, *27*, 2831.
(22) Yamamoto, Y.; Suzuki, T.; Kaizaki, S. *J. Chem. Soc., Dalton Trans.* **2001**, 1566.
(23) Yoshioka, N.; Irisawa, M.; Abe, M.; Aoki, T.; Aizawa, N.; Inoue, H. *Mol. Cryst. Liq. Cryst.* **1997**, *306*, 397.
(24) Luneau, D.; Risoan, G.; Rey, P.; Grand, A.; Caneschi, A.; Gatteschi, D.; Laugier, J. *Inorg. Chem.* **1993**, *32*, 5616. Lewis, G. R.; Blake, A. J. *Acta Crystallogr. C*, **2002**, *58*, m398.

the presence of ferromagnetic intra- and intermolecular interactions. We assume that there is a secondary weak intermolecular interaction which would be antiferromagnetic, while the major intermolecular interaction is ferromagnetic. The metamagnetic structure may be described as interchain antiferromagnetic coupling among ferromagnetically correlated chains[25,26] or as intersheet antiferromagnetic coupling among ferromagnetically correlated sheets.[27,28] As the X-ray crystallographic analysis revealed, the H-bonds are found in two directions, $a + b$ and $a - b$, forming a two-dimensional network (Figure 2b). We have to think that the interaction of the sheet structure parallel to the *ab* plane (J_{ab}) is ferromagnetic and that the intersheet interaction (J_c) is antiferromagnetic. The J_c is very small and origins of J_c can hardly be discussed, but mechanisms of J_{ab} are worth being discussed based on the structure determined.

The spin-polarization mechanism[29] may be operative in pathways through the contacts O2···H1# and O2···H3#, namely, N3#(↑)−C4#(↓)−C2#(↑)−C3#(↓)−N2#(↑)−H3#(↓)···O2(↑) or N3#(↑)−C4#(↓)−C2#(↑)−N1#(↓)−C1#(↑)−H1#(↓)···O2(↑). However, it has not been established whether the spin polarization originally developed on alternant hydrocarbons can be applied to heteroaromatic and five-membered imidazole rings, although the magnetic couplings through thiophene,[30] pyridine,[31] and phenol[5] groups were interpreted in terms of the spin polarization. A superexchange interaction along Ni−imidazole···O2# is also taken into consideration. Another possible explanation is as follows. The singly occupied molecular orbital (SOMO) is highly localized at the N−O group in NN compounds while the next highest occupied molecular orbital (NHOMO) is delocalized over the whole molecule, as confirmed by the UHF/PM3 calculation[32] using the determined geometry from the ligand portion in **3**. Awaga and co-workers proposed[33] that the ferromagnetic intermolecular exchange interaction in *β*-*p*-nitrophenyl NN was brought about from the conditions that intermolecular SOMO−SOMO overlap was negligible while SOMO−NHOMO overlap was substantial, which requires accordingly the proximity between the NN group and the *p*-nitrophenyl group in an adjacent molecule. This interpretation seems to hold for the present complexes (**1**−**4**). The NN group and imidazole ring are located closely and connected with the H-bonds, while the NN groups are apart from each other, thus leading to ferromagnetic coupling between the NN spins. It should be noted that these geometries can be realized by the H-bonds between the axial ligand and the imidazole NH proton in a side-by-side and head-to-tail manner.

The shortest interatomic distance is found between nitrate oxygen and imidazole hydrogen atoms. In contrast to the NN···imidazole contacts described above, the magnetic interaction through the nitrate···imidazole contacts seems to be very small because the contacting atoms carry only polarized spin density, which is supposed to be very small. McConnell proposed that the magnetic coupling is proportional to the product of the spin densities at contacting atoms ($H_{AB} = -S_A \cdot S_B \Sigma J_{ij} \rho_i^A \rho_j^B$).[34] Nevertheless, the H-bond character in the nitrate···imidazole contacts plays an important role in the molecular packing viewing from the extremely short interatomic distance.

The double H-bonds described as [−M−X(axial ligand)···H_{ImH}−]$_2$ for **5** and **12** (Figure 3) forms a macrocyclic structure which contains two imidazole rings. These imidazole rings are arranged in a parallel manner, owing to the symmetry. A mechanism for magnetic interaction in aromatic radicals was proposed by McConnell[34] and experimentally verified using a paracyclophane skeleton and a pancake-type aromatic dimer.[35] A through-space $\pi-\pi$ interaction between the imidazole rings may bring about magnetic interactions.

We found the intermolecular ferromagnetic interaction in the series of [M(4ImNNH)$_2$X$_2$] (M = Mn, Co, Ni, Cu; X = NO_3, Cl, Br) with high probability (7 cases out of 10 excluding **7** and **11** because of the diamagnetic ground states), as evidenced by the $\chi_{mol}T$ increase from the plateau defined by the ground state. The H-bonds in **1**−**4** are concluded to afford ferromagnetic couplings and those in **5**−**12** may also provide ferromagnetic exchange pathways. Crystal designs involving H-bonds seem very important for the development of molecule-based magnetic materials.

Summary

A new radical chelating ligand 4ImNNH and new complexes **1**−**12** were prepared. Magnetic measurements revealed that the NN and nickel(II) spins in **3** were ferromagnetically correlated with $2J/k_B = 85$ K. Furthermore, **3** underwent a magnetic phase transition to become an antiferromagnet below 3.4 K and also exhibited a metamagnetic transition on applying a magnetic field of 5.5 kOe at 1.8 K. The two-dimensional ferromagnetic network is assumed, which is accompanied by two-strand H-bonds at

(25) Miller, J. S.; Zhang, J. H.; Reiff, W. M.; Dixon, D. A.; Preston, L. D.; Reis, A. H., Jr.; Gebert, E.; Extine, M.; Troup, J.; Epstein, A. J.; Ward, M. D. *J. Phys. Chem.* **1987**, *91*, 4344. Reiff, W. M.; Wong, H.; Foner, S.; Frankel, R. B.; Long, G. J. *J. Chem. Phys.* **1978**, *68*, 4781.

(26) Ishida, T.; Tomioka, K.; Nogami, T.; Yoshikawa, H.; Yasui, M.; Iwasaki, F.; Iwamura, H.; Takeda, N.; Ishikawa, M. *Chem. Phys. Lett.* **1995**, *247*, 7.

(27) Rabu, P.; Rueff, J. M.; Huang, Z. L.; Angelov, S.; Souletie, J.; Drillon, M. *Polyhedron* **2001**, *20*, 1677. Sekine, T.; Okuno, T.; Awaga, K. *Inorg. Chem.* **1998**, *37*, 2129. Monfort, M.; Resino, I.; Ribas, J.; Stoeckli-Evans, H. *Angew. Chem., Int. Ed.* **2000**, *39*, 191. Usuki, N.; Ohba, M.; Okawa, H. *Bull. Chem. Soc. Jpn.* **2002**, *75*, 1693.

(28) Benoit, A.; Flouquet, J.; Gillon, B.; Schweizer, J. *J. Magn. Magn. Mater.* **1983**, *31*−*34*, 1115. Ishida, T.; Ohira, S.; Watanabe, I.; Nogami, T.; Nagamine, K. *Polyhedron* **2001**, *20*, 1551.

(29) Iwamura, H. *Adv. Phys. Org. Chem.* **1990**, *26*, 179. Rajca, A. *Chem. Rev.* **1994**, *94*, 871. Longuet-Higgins, J. C. *J. Chem. Phys.* **1950**, *18*, 265. Crayston, J. A.; Devine, J. N.; Walton, J. C. *Tetrahedron* **2000**, *56*, 7829.

(30) Akita, T.; Mazaki, Y.; Kobayashi, K.; Koga, N.; Iwamura, H. *J. Org. Chem.* **1995**, *60*, 2092.

(31) Kumada, H.; Sakane, A.; Koga, N.; Iwamura, H. *J. Chem. Soc., Dalton, Trans.* **2000**, 911. Kitano, M.; Ishimaru, Y.; Inoue, K.; Koga, N.; Iwamura, H. *Inorg. Chem.* **1994**, *33*, 6012. Ishimaru, Y.; Kitano, M.; Kumada, H.; Koga, N.; Iwamura, H. *Inorg. Chem.* **1998**, *37*, 2273.

(32) Stewart, J. J. P. MOPAC ver 6.0, *QCPE* #455.

(33) Awaga, K.; Inabe, T.; Maruyama, Y. *Chem. Phys. Lett.* **1992**, *190*, 349. Awaga, K. In *Magnetic Properties of Organic Materials*; Lahti, P. M., Ed.; Marcel Dekker: New York, 1999; Chapter 25, pp 519−534.

(34) McConnell, *J. Chem. Phys.* **1963**, *39*, 1910.

(35) Izuoka, A.; Murata, S.; Sugawara, T.; Iwamura, H. *J. Am. Chem. Soc.* **1985**, *107*, 1786. Imachi, R.; Ishida, T.; Suzuki, M.; Yasui, M.; Iwasaki, F.; Nogami, T. *Chem. Lett.* **1997**, 743.

the NN···imidazole contact and at the nitrate···imidazole contacts. Although both intra- and intermolecular magnetic exchange couplings are dominantly ferromagnetic for **3**, the magnetic ground state is concluded to be antiferromagnetic owing to antiferromagnetic coupling ascribable to the weak intersheet interaction. There are two categories of molecular-based magnets: ferrimagnets and ferromagnets. Rey and coworkers reported the ferrimagnets containing two-dimensional networks by use of the 2ImNN anion and manganese(II) ion.[10] We can propose a strategy toward *ferro*magnets containing an anionic 4ImNN and nickel(II) cation via the deprotonation process from **3** and, even when the 2ImNN anion or copper(II) ion is available, ferromagnets can also be expected because the chelate six-membered ring may favor a planar structure by using less bulky imidazole groups. Furthermore, the deprotonation will give rise to higher dimensionality due to the imidazolate bridges and magnetically dense systems because of the purge of bulky anions, probably leading to high ordering temperatures. Preparation of polymeric [M(4ImNN)$_2$] (M = Ni, Cu) solids as genuine ferromagnetic molecular materials is now underway.

Acknowledgment. This work was supported by a Grant-in-Aid for Scientific Research on Priority Areas of "Molecular Conductors and Magnets" (No. 730/11224204) and by a Grant-in-Aid for Scientific Research (No. 13640575), both from the Ministry of Education, Culture, Sports, Science and Technology, Japan.

Supporting Information Available: Crystallographic information files and ortep drawings of new compounds, 4ImNNH, **1**−**4**, **5**, and **12** and supplementary Figures S1−S3. This material is available free of charge via the Internet at http://pubs.acs.org.

IC0349048